ISSN 1726-5479

SENSORS & TRANSDUCERS

12/10 vol. 123

Sensor Market Trends

International Frequency Sensor Association Publishing

IFSA

Sensors & Transducers

Volume 123, Issue 12, December 2010 www.sensorsportal.com **ISSN 1726-5479**

Sensors & Transducers Journal (ISSN 1726-5479) is a peer review international journal published monthly online by International Frequency Sensor Association (IFSA).

Sensors & Transducers Journal

Contents

Volume 123
Issue 12
December 2010

www.sensorsportal.com

ISSN 1726-5479

Research Articles

Authors are encouraged to submit article in MS Word (doc) and Acrobat (pdf) formats by e-mail: editor@sensorsportal.com
Please visit journal's webpage with preparation instructions: http://www.sensorsportal.com/HTML/DIGEST/Submition.htm

The Third International Conference
on Bioinformatics, Biocomputational Systems and Biotechnologies

BIOTECHNO 2011

May 22-27, 2011 - Venice, Italy

www.sensorsportal.com

Tracks:

A. Bioinformatics, chemoinformatics, neuroinformatics and applications
- Bioinformatics
- Advanced biocomputation technologies
- Chemoinformatics
- Bioimaging
- Neuroinformatics

B. Computational systems
- Bio-ontologies and semantics
- Biocomputing
- Genetics
- Molecular and Cellular Biology
- Microbiology

C. Biotechnologies and biomanufacturing
- Fundamentals in biotechnologies
- Biodevices
- Biomedical technologies
- Biological technologies
- Biomanufacturing

Important deadlines:

Submission (full paper)	January 10, 2011
Notification	February 20, 2011
Registration	March 5, 2011
Camera ready	March 20, 2011

http://www.iaria.org/conferences2011/BIOTECHNO11.html

The Seventh International Conference
on Networking and Services

ICNS 2011

May 22-27, 2011 - Venice, Italy

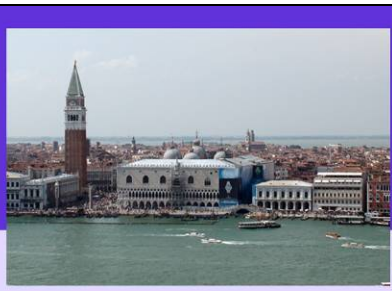

www.sensorsportal.com

Important deadlines:

Submission (full paper)	January 10, 2011
Notification	February 20, 2011
Registration	March 5, 2011
Camera ready	March 20, 2011

http://www.iaria.org/conferences2011/ICNS11.html

Tracks:
- ENCOT: Emerging Network Communications and Technologies
- COMAN: Network Control and Management
- SERVI: Multi-technology service deployment and assurance
- NGNUS: Next Generation Networks and Ubiquitous Services
- MPQSI: Multi Provider QoS/SLA Internetworking
- GRIDNS: Grid Networks and Services
- EDNA: Emergency Services and Disaster Recovery of Networks and Applications
- IPv6DFI: Deploying the Future Infrastructure
- IPDy: Internet Packet Dynamics
- GOBS: GRID over Optical Burst Switching Networks

The Sixth International Conference on Systems

ICONS 2011

January 23-28, 2011 - St. Maarten,
The Netherlands Antilles

www.sensorsportal.com

Important deadlines:

Submission (full paper)	September 25, 2010
Notification	October 20, 2010
Registration	November 5, 2010
Camera ready	November 5, 2010

http://www.iaria.org/conferences2011/ICONS11.html

Tracks:
- Systems' theory and practice
- System engineering
- System instrumentation
- Embedded systems and systems-on-the-chip
- Target-oriented systems [emulation, simulation, prediction, etc.]
- Specialized systems [sensor-based, mobile, multimedia, biometrics, etc.]
- Validation systems
- Security and protection systems
- Advanced systems [expert, tutoring, self-adapting, interactive, etc.]
- Application-oriented systems [content, eHealth, radar, financial, vehicular, etc.]
- Safety in industrial systems
- Complex Systems

Sensors & Transducers Journal, Vol. 123, Issue 12, December 2010, pp. 1-15

Sensors & Transducers

ISSN 1726-5479

http://www.sensorsportal.com

Development of Electromechanical Architectures for AC Voltage Metrology

[1]Alexandre BOUNOUH, [1]François BLARD, [2, 3]Henri CAMON, [1]Denis BELIERES
[1] LNE – 29 avenue Roger Hennequin, 78197 Trappes, France
[2] CNRS-LAAS, 7 avenue du colonel Roche, F-31077 Toulouse, France
[3] Université de Toulouse; UPS, INSA, INP, ISAE; LAAS; F-31077 Toulouse, France
E-mail: alexandre.bounouh@lne.fr, camon@laas.fr

Received: 22 July 2010 /Accepted: 21 December 2010 /Published: 28 December 2010

Abstract: This paper presents results of work undertaken for exploring MEMS capabilities to fabricate AC voltage references for electrical metrology and high precision instrumentation through the mechanical-electrical coupling in MEMS. From first MEMS test structures previously realized, a second set of devices with improved characteristics has been developed and fabricated with Silicon on Insulator (SOI) Surface Micromachining process. These MEMS exhibit pull-in voltages of 5 V and 10 V to match with the best performance of the read-out electronics developed for driving the MEMS. Deep Level Transient Spectroscopy measurements carried out on the new design show resonance frequencies of about only some kHz, and the stability of the MEMS output voltage measured at 100 kHz has been found very promising for the best samples where the relative deviation from the mean value over almost 12 hours showed a standard deviation of about 6.3 ppm. *Copyright © 2010 IFSA.*

Keywords: MEMS Design, SOI Process, Electrical metrology, Voltage Reference.

1. Introduction

MEMS technologies have increasingly developed since the Seventies thanks to the capacity of intelligent assembly of basic devices (beams, springs, wheels, gears…) to manufacture complex Microsystems (engine, resonators, actuators, pumps…). From MEMS devices made of membranes, beams or seesaw structures, the first applications in electrical metrology have emerged around 1995 with the first AC-DC converters where the principle is to balance two electrical forces generated by AC and DC voltages [1, 2]. Afterwards, several other applications have been proposed: AC and DC voltage references [3-6], AC-DC converters [7, 8], current reference and low frequency voltage divider

[9, 10], and RF and microwaves power sensors [11-13]. Such devices are made of micro-machined electrodes of which one at least is movable thanks to the application of an electrostatic force between the two electrodes, inversely proportional to the square of the gap. For voltage references, one uses in such a Microsystem of variable capacitor (Fig. 1) the "pull-in" effect, which limits in DC actuation the stable displacement x of the movable electrode to the third of the gap d. In the characteristic voltage-displacement of Fig. 1, the pull-in voltage V_{pi} corresponds to the maximum voltage applied to the MEMS beyond which the two electrodes are put abruptly in contact.

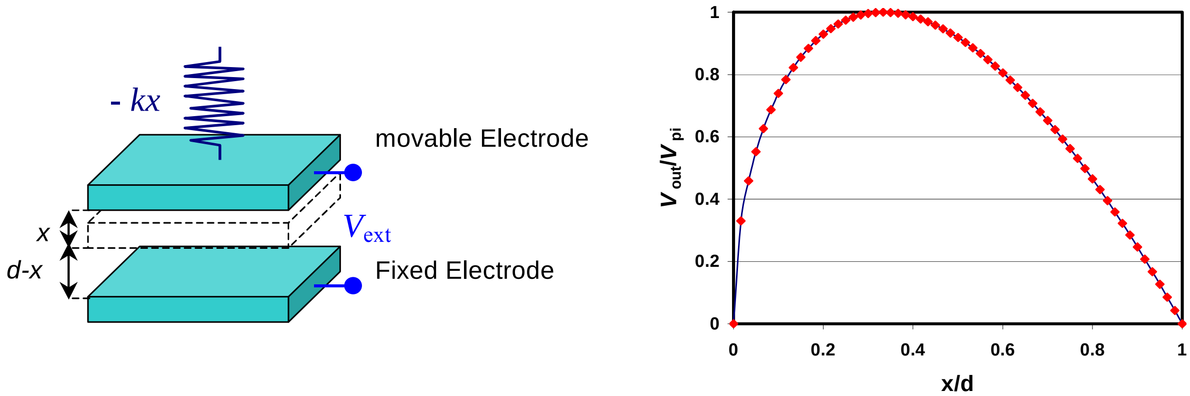

Fig. 1. Variable MEMS capacitor and its calculated voltage-displacement characteristic.

As this point is an *extremum*, it can be used as a stable DC voltage reference (the relative variation of V_{pi} is only proportional to the square of the relative variation of the displacement). However, in DC voltage actuation, specific techniques and feedback electronics are needed to stabilize the mobile electrode at the pull-in point [14-19].

If the previous structure is now biased with an AC sinusoidal current of amplitude I_{RMS} and frequency ω, the AC voltage presents, according to the current I_{RMS}, a maximume equal to V_{pi}:

$$V_{AC}^{\max} = V_{pi} = \sqrt{8kd^2 / 27C_0}\,, \tag{1}$$

where C_0 is the capacitance at $x = 0$ and k the spring constant (Fig. 2).

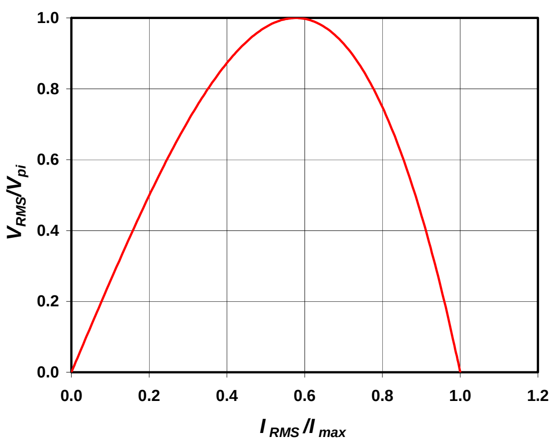

Fig. 2. MEMS output Voltage versus I_{RMS} biasing current, I_{max} being the maximum effective current flowing in the MEMS.

This point of maximum voltage can be used as a stable AC voltage reference since its relative variation in this point depends only on the square of the relative variation of the current:

$$\Delta V_{RMS}/V_{pi} \sim -3/2\ (\Delta I/I_{RMS\text{-}max})^2, \quad (2)$$

where $I_{RMS\text{-}max}$ corresponds to the current at V_{pi}. Of course, the frequency of the current should be much higher than the mechanical resonance frequency of the MEMS in order to minimize the influence of the mechanical forces.

The pull-in effect approach was already utilized for the development of stable MEMS components [20, 21]. In this work, an AC voltage reference based on a commercial MEMS accelerometer showed stability at 100 kHz of about 2 ppm over three weeks. This stability has been obtained by applying corrections to the raw measurements due to temperature, humidity and pressure effects, but primarily by the compensation of the temperature dependent DC built-in voltage generated at metal-semiconductor interfaces in the system.

The stability of the MEMS voltage standards based on the pull-in effect depends on the stability of the spring constant k and the geometrical dimensions of the MEMS defining the gap d and the nominal capacitance. For this purpose, a monocrystal of silicon is used for manufacturing these systems (the basic concept is the electromechanical transduction in MEMS in which the high mechanical stability of a single crystal of silicon would be transferred to an electrical stability through the mechanical-electrical coupling). However, a temperature regulation of the MEMS is then needed to control the temperature dependence of the spring constant which is induced by the variation with the temperature of Young's modulus in silicon crystal. Two others phenomena could be a limitation to the MEMS voltage stability: native mechanical stresses in the material or induced by the manufacture processes of the MEMS components (assembly and packaging) and charge effects of the silicon surfaces. Therefore, in order to have the required stability for primary and secondary metrology fields and precision instrumentation, special designs and architectures featuring low sensitivity with respect to strain and geometrical dispersion have to be investigated, as well as technological processes featuring low residual stress and high repeatability.

The work presented in this paper is aiming at developing AC voltage references for metrology and precision instrumentation. From first MEMS test structures (design N°1) previously realized [22, 23], a second set of devices with improved characteristics (design N°2) has been developed and fabricated with a Silicon On Insulator (SOI) Surface Micromachining process. Moreover, two specific read-out electronics for driving the MEMS have been studied and completely realized. Deep Level Transient Spectroscopy measurements were carried out to study the dynamical behaviour of the devices and to determine their mechanical resonance frequencies. Finally, the stability of the MEMS output voltage of the structures has been evaluated and led to rethink the devices architecture itself to match with the constraints of the SOI process.

2. Design of the MEMS Devices

The patterns of the Microsystems must be chosen by taking into account the following parameters: *i*) the value of the variable capacitor that should be greater than the parasitic capacitances of the system with a variation consistent with the detection of the pull-in voltage; *ii*) the targeted pull-in point that defines the value of the voltage reference; *iii*) the mechanical resonance frequency that must be sufficiently low, *iv*) the technological process itself.

2.1. Design N°1

The first MEMS design was aiming at assessing, on one hand the capabilities and performance of an industrial SOI process, and on the other hand specific MEMS architectures for AC voltage references. These MEMS were designed by using a finite element software (CoventorWare) on the basis of a silicon disk plate (movable membrane) featuring different configuration of the suspending springs on the substrate (fixed electrode) to ensure a controlled vertical piston mode motion [22, 23]. Fig. 3 shows the layouts of the movable part of these structures. The first device named **A** is a 500 µm-radius disk plate with three curved springs of 1300 µm long and 10 µm width. Device **B** is very similar to the sample **A** and has the same dimensions, only the curved part of the springs in **B** are attached together forming a released ring of 10 µm width, which slightly increases the stiffness of the structure and then V_{pi}. The aim of this design is to improve the vertical guidance of the movable plate. The same disk plate as previously (r = 500 µm) is used for forming the last device named **C** having four straight springs (360 µm × 10 µm).

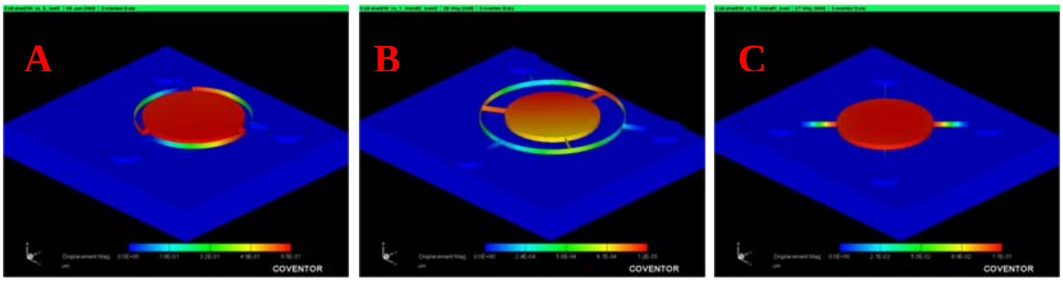

Fig. 3. Layouts of MEMS test structures of the design N°1 modelled with CoventorWare.

The computations are performed with the electromechanical formulation of CoventorWare. The pull-in voltage of each device is calculated through the computation of the displacement x of the membrane due to the application of an electrostatic force generated by the bias voltage applied between the two electrodes formed by the movable membrane and the substrate. The simulations are carried out by taking into account the exact dimensions of the SOI wafer and particularly the gap d of 2 µm. In this case, the voltage corresponding to the membrane displacement of 0.66 µm (d/3) gives an estimation of the pull-in voltage. From these results, one can then calculate for each structure the stiffness k of the springs and the resonance frequency f_0. The targeted pull-in voltages are ranging from 2 V to 90 V.

2.2. Design N°2

The second set of MEMS structures has been designed with the aim to get samples having high nominal capacitances compared to the parasitic ones and lower pull-in voltages. The objective is the evaluation of the intrinsic stability of the MEMS capacitors without being limited by the electronics noises. Indeed, in the case of AC voltage references, the MEMS are put in the feedback loop of a precision amplifier consisting in a voltage-to-current converter. This amplifier should have a great product gain-bandwidth to work up to some hundreds kHz, and the most powerful amplifiers available have voltage supply limited to about ±18 V at most. Hence, two MEMS structures **E** and **F** corresponding to the design N°2 have been developed to have pull-in voltages of 5 V and 10 V respectively. The layout of the design N°2 is depicted in Fig. 4. It is based on a silicon disk plate with three straight suspending springs. In this design the nominal capacitance of the movable part is much higher than the parasitic capacitance induced by the anchorage points, which are now of small size, and the contact pads limited here to just one electrical contact. The value of the movable capacitor is now of 23 pF against 5 pF for the design N°1. Moreover, the structures are guarded by a silicon ring of

65 µm width to avoid the effect of any leakage currents. The dimensions of the two MEMS are given in Table 1 and both structures have been modelled with CoventorWare. The calculated parameters of the two structures **E** and **F** are summarized in Table 2 where the capacitance C_0 at x=0, the spring constant k, the resonance frequency and the pull-in voltage are given.

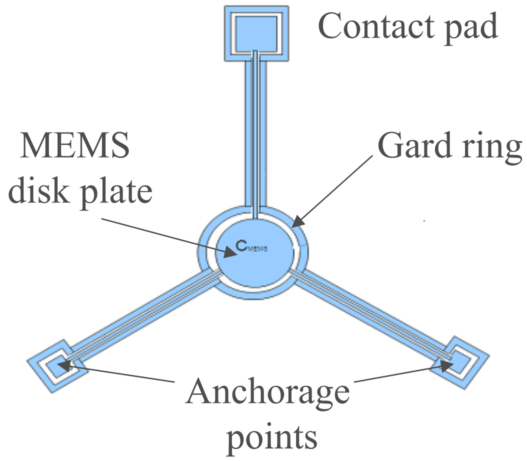

Fig. 4. MEMS design N°2 used for the **E** and **F** samples.

Table 1. Dimensions of the MEMS devices of the design N°2.

MEMS	Diameter (µm)	Length (µm)	Width (µm)
E	2210	1072	10
F	2210	884	10

Table 2. Calculated MEMS characteristics of the design N°2.

MEMS	C_0 (pF)	k (N/m)	f_0 (kHz)	V_{pi} (V)
E	22.8	1437	10	5.5
F	22.8	437	18	10

3. MEMS Fabrication

The choice of the technological process has been driven by the theoretical considerations of the previous sections where it is very important to have a technology which minimizes the gradient of stress and that allows a good control of the dimensions. We have chosen a Silicon On Insulator (SOI) surface micromachining process and a Multi-project Wafer (MPW) of an industrial foundry (Tronic's Microsystems) to make sure that the process will be repeatable. The SOI top layer is a 60 µm thick monocrystalline silicon layer used for the mechanically active layer, exhibiting excellent mechanical characteristics (it can tolerate up to 10^{10} cycles without any crack or fatigue [24]). The silicon dioxide layer acting as insulator and spacer defines the gap of 2 µm and the silicon substrate of 450 µm thick acting as the fixed electrode. Silicon wafers resistivity is in the range of 0.02 Ω.cm obtained by a high boron p-type doping of 2.10^{18} cm^{-3}.

Fig. 5 illustrates the process flow used for the realizations of our structures. The top layer is first etched in order to realize the disk plate suspended with springs and then gold contact pads are realized. After the partial selective etching of the silicon dioxide, the plate and the springs are released from the substrate.

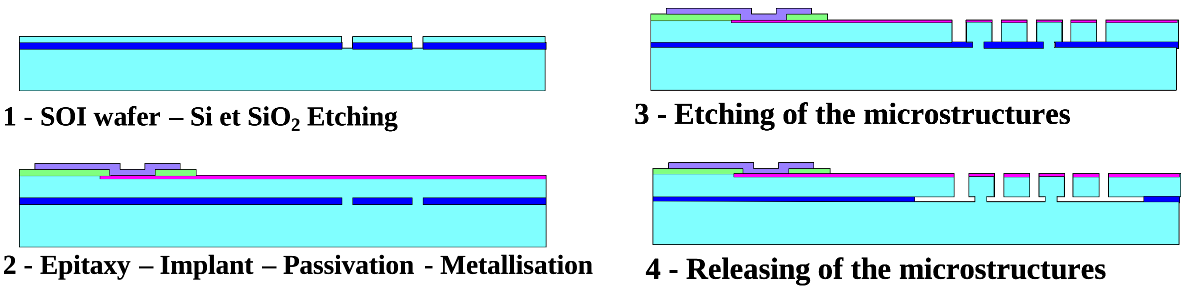

Fig. 5. SOI process flow of Tronic's Microsystems used for MEMS fabrication.

To ensure the stability of the MEMS, a vacuum hermetic silicon wafer level packaging protects the die. The final structure is composed by the assembly of the SOI wafer where the MEMS is realized and a silicon wafer acting as a cap for protecting the MEMS. The non-sealed areas are defined by partial etch of a silicon dioxide initially realized and the metallization define the sealing areas for assembly. After assembly, via holes are realized to allow electrical contact of the structure to the pads.

Tronic's process has been used for elaborating our MEMS devices. Fig. 6 shows photos of the three fabricated MEMS of the design N°1 (**A**, **B** and **C**). To control the quality of the micromachining and etching processes, test patterns were realized on the same silicon wafer in the shape of beams and gaps of 3 µm and 4 µm width respectively. Measurements of these parameters over a dozen of samples corresponding to a dozen of dies, show a dispersion of less than 0.2 µm, which indicates a very good technology process control and an excellent repeatability.

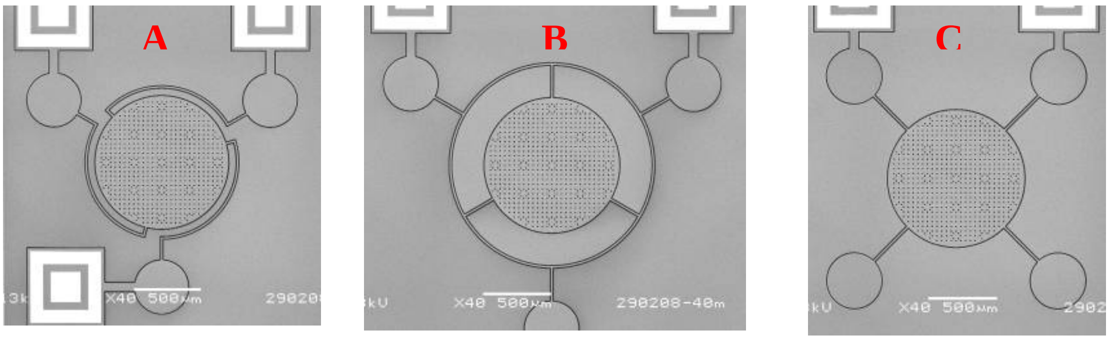

Fig. 6. SEM photos of the MEMS **A**, **B** and **C** fabricated following the design N°1.

With this same MPW Tronic's process, we have then fabricated structures following the design N°2 where the silicon membrane is fitted with a guard ring which can be put to a chosen electrical potential. Fig. 7 shows a SEM photo of a chip containing the two MEMS devices **E** (5 V) and **F** (10 V); sealed and not sealed dies have been fabricated. For each MEMS, there are several contact pads corresponding to the movable electrode, the guard, the silicon cap protecting the die and the silicon substrate. Let us note that for the hermetic dies, the pads are larger and contribute more in the total capacitance of the MEMS.

In the two previous technological runs, for each kind of MEMS architecture, we have produced 22 dies corresponding in total to 220 samples.

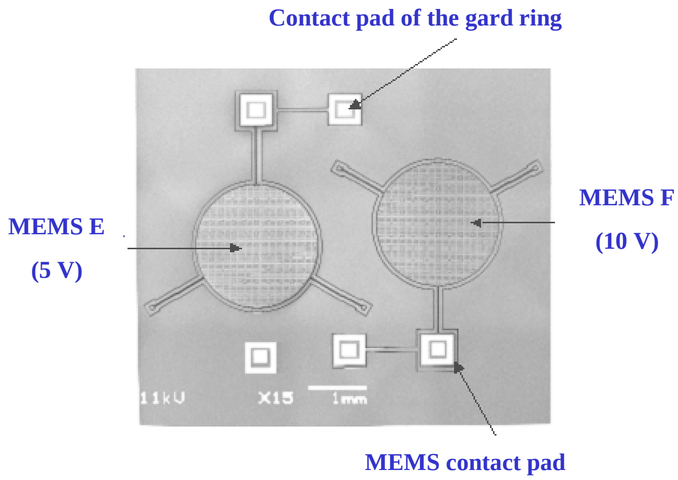

Fig. 7. SEM photo of a die containing both **E** and **F** MEMS structures fabricated following the design N°2.

4. Read-out Electronics

The principle of actuation of capacitive MEMS for the AC voltage reference needs relatively simple electronics. However, it must be carefully designed to avoid parasitic noises, given the values of the MEMS capacitance compared to the stray capacitance of the system itself (few pF). To drive the MEMS to the pull-in voltage for defining the AC voltage reference, we have developed two read-out electronics: a circuit stabilized by the MEMS capacitance but whose gain adjustment is manual, and a more sophisticated system that can automatically adjust the output voltage of the MEMS to its maximum value.

The scheme of the first electronics is shown in Fig. 8. As the MEMS have to be biased with an AC current, they are put in the feedback loop of amplifier A1 consisting in a voltage-to-current converter. Amplifier A1 should have a great product gain-bandwidth to work up to some hundreds of kHz. However, this kind of components has rarely small voltage offsets and polarization currents, then the low frequency precision amplifier A2 is used to fix the DC output voltage to zero.

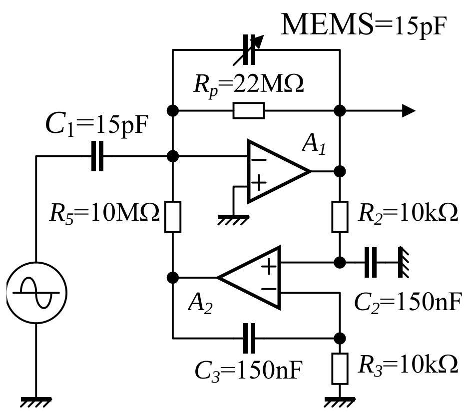

Fig. 8. Voltage-to-current read-out electronics.

To drive automatically the MEMS to the pull-in position, a proposed solution consists in controlling the operating point using an amplitude modulation (AM) of the RF signal, typically at 100 kHz, by a small sinusoidal signal at very low frequency. Indeed, such a feedback-loop eliminates many error sources, and the only remaining error is the amplifier gain. In this approach, a modulator performs the product of the input RF signal by the sum of a DC voltage and a small ac voltage. This signal has average amplitude that depends on the DC voltage, and a small depth amplitude modulation. If the average amplitude is correct, there is no very low frequency component in the amplitude of the detected output signal (except a residual signal at double of the modulating frequency). If there is a positive or a negative error, an AC voltage at very low frequency appears in phase or in opposite phase with the modulating signal (slope change in the *U-I* characteristic). A synchronous detection and a low pass filter allow to obtain an error voltage, which after integration constitutes the voltage control. In our case, we have applied the amplitude modulation detection by using a square-modulating signal instead of a sinusoidal wave. With such a modulation called ASK (Amplitude Shift Keyed), the current takes only two fixed values $I_{pi} \pm \Delta_I$ (the operating point no longer describes the arc of the *U-I* characteristic), and there is no residual modulation at double of the modulating frequency. This new approach has two advantages:

- There is no problem with sampled systems or pulses.

- The filtering circuits become very simple and therefore provide less phase shift in the loop.

For the same modulating frequency in both cases (sinusoidal and square modulating signals), the loop bandwidth can be greater. Moreover, instead of adding the modulating signal and the integrated control voltage, it has to be multiplied by the chosen modulation envelope and then to modulate the signal with this product. With a modulating sinusoidal, this requires an additional multiplier. With a square wave, the product is made with a simple CMOS analog switch, followed by a low-pass filter to control the harmonic content of the modulating signal. The synchronous demodulator is an analog switch, much more stable in DC current than an analog multiplier. Fig. 9 presents the block diagram of the AM electronic module for the AC voltage reference and shows the third generation AM electronics which integrates a temperature regulation of the MEMS by using small Peltier modules ensuring temperature stability at some mK.

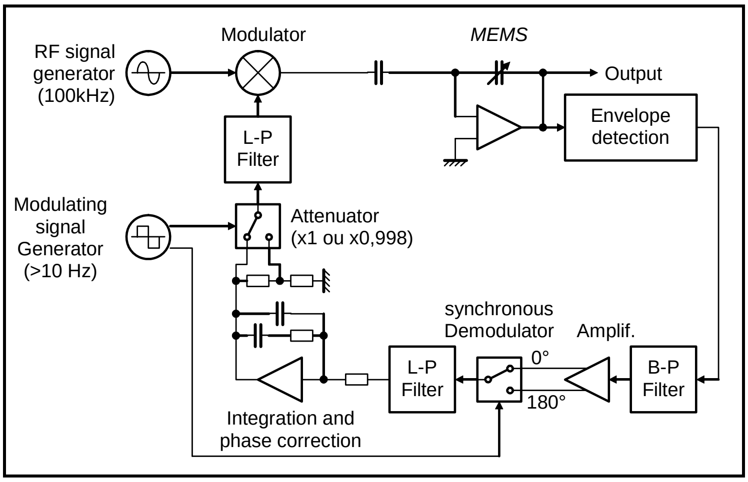

(a)

(b)

Fig. 9. Block diagram and photo of the AM electronics module integrating a temperature regulation of the MEMS with Peltier modules.

5. Measurements Results

5.1. Design N°1

First *C-V* curves have been carried out on the MEMS of the structure **A** by using a LCR-meter. An external DC bias voltage is applied to the MEMS and the capacitance is measured with an AC voltage of 0.1 V at 100 kHz. Fig. 10a shows the *C-V* characteristic of the structure **A** at 100 kHz for a bias voltage ranging from -2.5 V to 2.5 V. This *C-V* characteristic is quite symmetrical in positive and negative bias voltages. Indeed, the shift of the curve relatively to the zero voltage is only of tens of mV, reflecting an extremely low built-in voltage compared with samples from the literature showing built-in voltages up to 0.8 V [20]. In this case, the electrodes were metal coated, which is not the case for our devices. Furthermore, one can see clearly a pull-in effect occurring at V_{pi} = 1.96 V (and a pull-out voltage around 0.7 V) in a good agreement with the calculated value of 1.4 V made by ConventorWare. The same results on the pull-in voltages measured and calculated have been obtained on the other test structures (**B** and **C**).

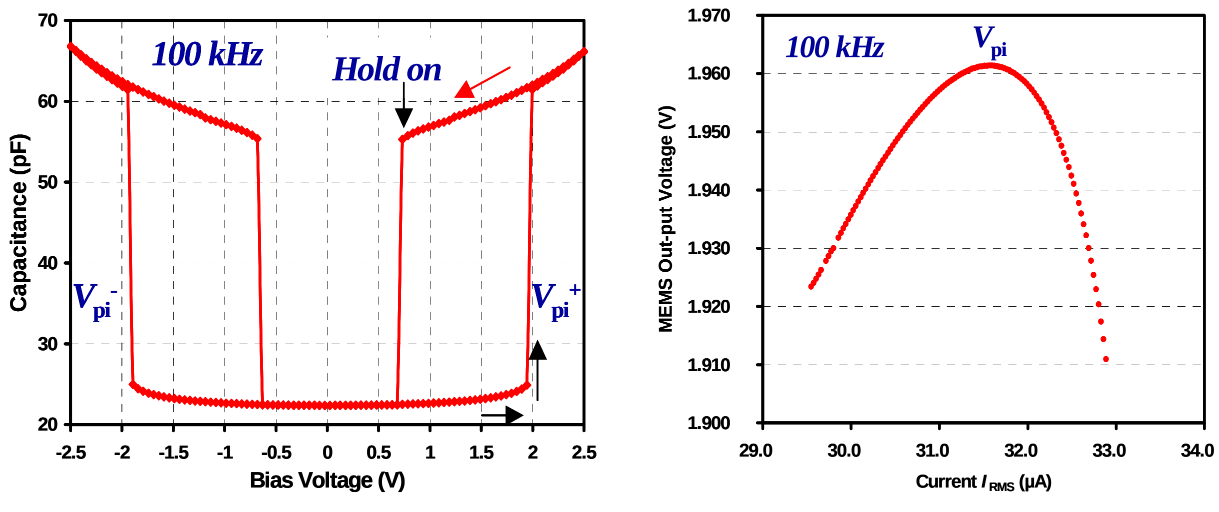

Fig. 10. *C-V* (a) and *U-I* (b) characteristics of the MEMS **A** at 100 kHz.

Measurements of the MEMS output RMS voltage according to the current I_{RMS} flowing in the MEMS (*U-I* characteristic) have been carried out at frequencies ranging from 10 kHz to 200 kHz. Fig. 10b displays the characteristic of the structure **A** at 100 kHz. All the other curves show the same maximum of the output voltage corresponding exactly to the pull-in voltage *V*pi = 1.96 V observed in the *C-V* curve.

The objectives of this first step and the test structures of the design N°1 were to assess the ability of finite element software to design specific architectures, the capabilities of an industrial MEMS SOI process for the fabrication and to develop read-out electronics. The evaluation of the whole set of devices of the design N°1 allows us to collect information and to make the following recommendations that will be used to design next generations of MEMS and have been followed for the design N°2:

- We have had many failures with MEMS having curved springs (samples **A**). Consequently, only structures with straight springs have to be considered in making the design N°2, which makes it possible to better predict the characteristics of the devices by modelling and analytical calculations.

- Limiting the number of electrical contact pads and reducing the size of the anchorage points of the movable electrode on the silicon substrate should significantly reduce the parasitic capacitances. We may also consider increasing the nominal capacitance by taking into account the limitations imposed by the rules of Tronic's process.
- To develop a precision electronics for driving the MEMS by using the best electronic components available and especially the main amplifier, one must work with MEMS structures with pull-in voltages below 20 V, ideally between 1 V and 10 V. This will enable an effective assessment of the intrinsic stability of the MEMS without being hindered by the electronics instabilities.
- To reduce the number of MEMS components per chip to avoid possible interactions and to ensure that all the different parts of the chip (inactive silicon, protecting cap) are put to a suitable potential by making dedicated contact pads.

5.2. Design N°2

The devices of this design have been realized by taking into account the previous remarks. Fig. 11a shows the *C-V* characteristic at 100 kHz of the structure E-HK11 corresponding to a MEMS **E** of the die named K11 sealed hermetically in vacuum. The nominal capacitance (at zero voltage) is 29 pF, which means that stray capacitances are of about 6 pF. The main part comes from the air-capacitance formed between the movable electrode and the silicon-covering cap that protects the MEMS. Indeed, the gap between these two parts is only of 5 μm and this capacitor is directly in parallel with the MEMS capacitor if both the substrate and the cap are grounded. Moreover, the shift of the center of the *C-V* curve corresponding to the built-in voltage is only of some tens of mV. This value is much lower in our devices compared to samples with metalized electrodes; the only contribution to the built-in voltage in our systems comes from the silicon-gold interface of the contact pads. The value of the pull-in voltage determined from Fig. 11a is of 4.095 V for this sample when the simulated value for these structures is of 5.5 V. Let us note that the dispersion of the pull-in voltage over several tested **E** samples is of a few tenths of volts.

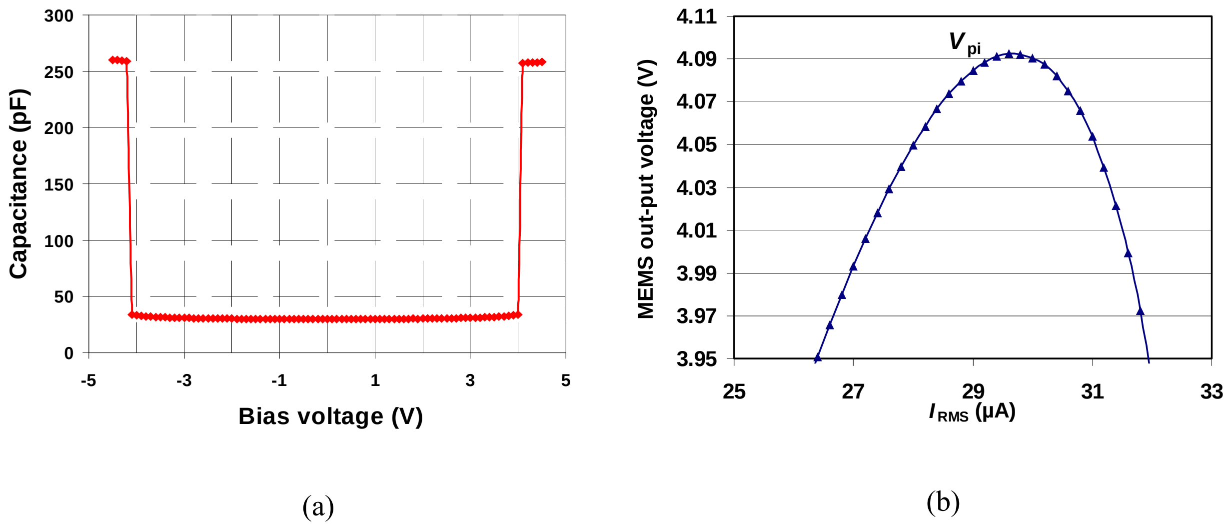

Fig. 11. *C-V* (a) and *U-I (b)* characteristics of the E-HK11 MEMS at 100 kHz.

The RMS output voltage of E-HK11 sample according to the driving current at 100 kHz is shown in Fig. 11b. The value of maximum voltage is of 4.095 V and corresponds exactly to the pull-in voltage previously determined. This point will define the value of the MEMS AC voltage reference whose stability must be fully evaluated and characterized according to environmental conditions.

For the MEMS of the structure **F**, the measured pull-in voltages are about 8 V, which corresponds to the same relative difference between the simulated and measured pull-in values for both types of samples. This discrepancy is due to a no optimized mesh of the structures and a low computation precision used in the software to reduce the computation time. The problem has been solved for an other run of fabrication not presented in this paper where the deviation between the simulated and measured pull-in voltages has been reduced to some %, which gives us best capabilities to simulate complex components.

Deep Level Transient Spectroscopy (DLTS) measurements have been carried out on these MEMS to analyze the dynamic behaviour of the movable plate by measuring the capacitance change in the time domain. Indeed, this technique allows to give information on the mechanical behaviour of Microsystems such as mechanical time responses, damping or resonance frequencies. Fig. 12 represents the response of E-HP11 MEMS to a DC voltage step of 3 V during 10 ms. The membrane oscillations represented by the oscillations of the MEMS capacitance are clearly observed over a time period lower than 5 ms beyond which the movable electrode becomes stable. Moreover, the membrane behaves in the same way when establishing and stopping the voltage step. This indicates that the system is not very damped which is consistent with the fact that the MEMS in HP11 die are hermetically sealed in a vacuum. The resonance frequency of the MEMS determined from the DLTS measurements is of about 2.8 kHz, which makes it possible to have AC voltage references working from about 30 kHz (ten times the resonance frequency).

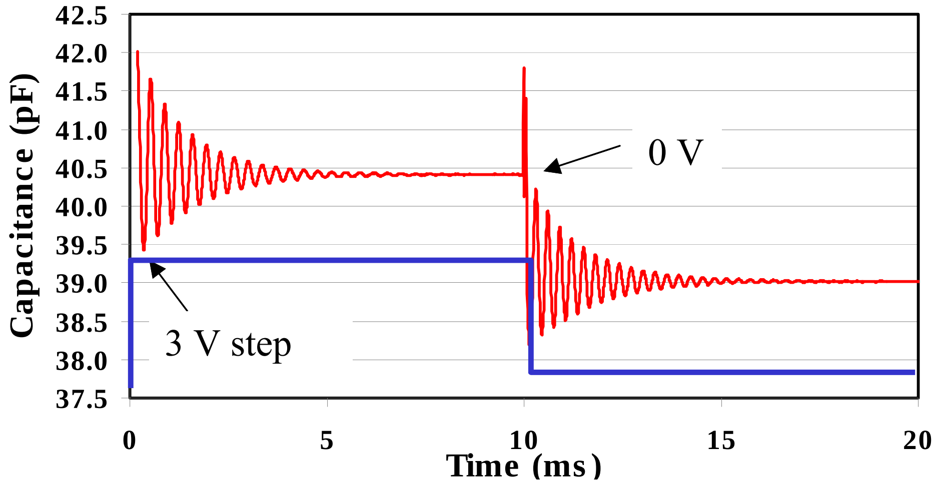

Fig. 12. DLTS measurements of the MEMS E-HP11 showing capacitance oscillations in the time domain when a voltage step of 3 V is applied.

The stability measurements of the AC voltage reference, corresponding to the maximum of the *U-I* curves, have been performed on several MEMS devices of the design N°2. The driving current is supplied by a precision calibrator (Fluke 5720A). The MEMS RMS output voltage is measured by a digital voltmeter (Agilent 3458A) put in the AC analogue mode with an integration time of 10 s. Moreover, the read-out electronics is fitted with temperature (T), relative humidity (HR) and pressure (P) sensors. These environment parameters have been kept as stable as possible and are measured simultaneously with the MEMS output voltage. Fig. 13 presents the relative deviation from the mean value of the output voltage of the E-HK6 MEMS (4 V nominal value) at 100 kHz over almost 12 hours and in the following conditions: 24.36 °C $< T <$ 24.37 °C, 43.2 % $< HR <$ 44.4 % and 995 hPa $< P <$ 999 hPa. The mean standard deviation (1σ) of the pull-in voltage measurements for this device is about 6.3 ppm, which is at 100 kHz, a very good result regarding the state of the art in AC voltage metrology where typical ac-dc differences of thermal converters are of some ppm at 100 kHz.

However, for this sample and for some others devices as well, this deviation can reach up to 30 ppm when the measurements are carried out continuously over longer times (several days).

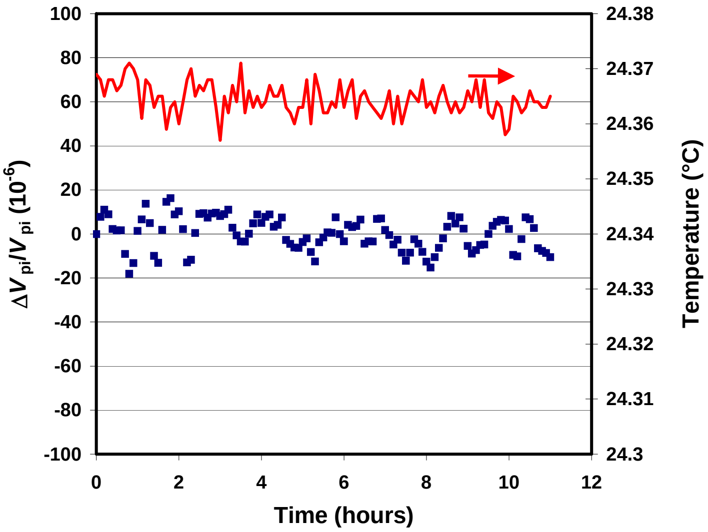

Fig. 13. Stability measurements of the RMS output voltage of E-HK6 sample.
The mean standard deviation (1σ) is of 6.3 ppm.

6. Discussions

The measured stability of our MEMS structures include the stability of the MEMS output voltage, which depends on the electronics performance and its noise level, and also the stability of the digital voltmeter put in the AC analogue mode and measuring at 100 kHz. However, this cannot explain the larger deviations observed when the measurements last longer. Several reasons could explain this behavior: first, the electrode surfaces of our structures are not metalized due to the SOI process used for the fabrication. This makes the built-in voltage negligible in our MEMS and its correction not applicable. However, even if the silicon is strongly doped to be conductive, a natural silicon oxide can be formed on the electrode surfaces, and electrical charges can then accumulate on these surface regions causing instabilities of the voltage across the MEMS capacitor. Secondly, the MEMS components are stuck on TO8 supports by using a conductive epoxy having electrical characteristics and mechanical behavior that are not optimized. Indeed, one of the electrical contacts of the MEMS capacitor is made through this epoxy since the SOI substrate is acting as the fixed electrode. An electrical resistor is therefore added in series with the MEMS capacitor and its variations will directly impact the output voltage of the feedback amplifier that defines the voltage reference. But from our point of view, the main reason that could explain the obtained results comes from the mismatch between the vertical motion chosen for the movable electrode and the dimensional characteristics of the SOI wafer imposed by the industrial Tronic's process, particularly the thickness of the silicon active layer of 60 µm. Indeed, to design MEMS structures with targeted pull-in voltages about 10 V or less, this thickness of the SOI wafer lead to designed springs having typically 10 µm of widths. This configuration is not really convenient with a vertical displacement of the movable membrane: such springs profiles (10 µm in width according to **X**-axis and 60 µm in depth according to **Z**-axis) lead to an anisotropic stress and displacement behaviors with an easy axis along x direction corresponding to an in-plane (horizontal) displacement instead of a vertical motion. From this assumption and taking into account the possibilities of the available SOI Tronic's process, we have designed MEMS devices in which both electrodes (movable and fixed ones) are realized on the same silicon active layer in the shape of silicon split fingers as shown in Fig. 14. The displacement of the movable plate is now occurring in the plane of the system matching more with the spring dimensions. Full description and results of the characterizations and measurements of these devices will be published elsewhere. Let us just mention that the stability of the voltage references ranging from 2 V to 14 V has been strongly enhanced with this split fingers systems reaching about 1 ppm of standard deviation at a frequency of 100 kHz and over more than 150 hours of measuring time without any kind of error corrections on the raw data.

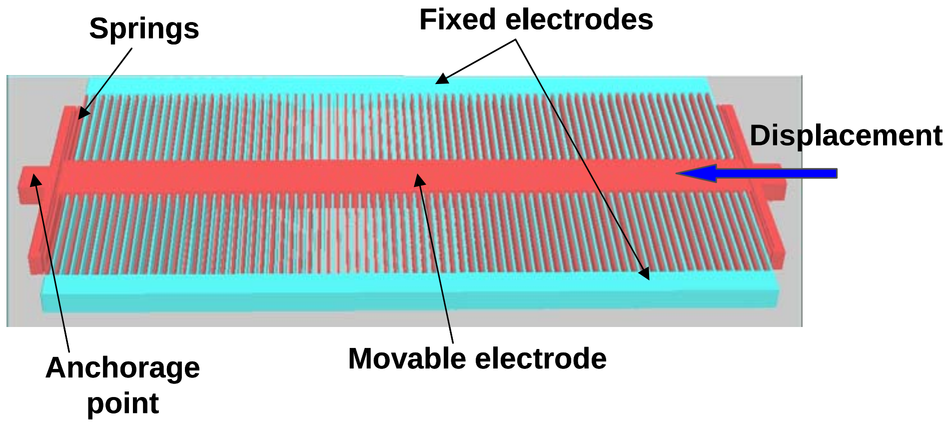

Fig. 14. Split fingers MEMS design with a lateral displacement of the movable electrode. The distance between two fingers of the fixed and movable electrodes defines the electrode gap.

7. Conclusion

This work was aiming at exploring MEMS architectures to fabricate AC voltage references by using the pull-in voltage approach. First test structures (design N°1) have been designed by finite element software and fabricated using a Silicon On Insulator Surface Micromachining process. The measured MEMS AC voltage reference values of these test structure have been found in a good agreement with the calculated values performed with CoventorWare. The objectives of this first work have been met in assessing the ability of the finite element software to design specific architectures, the capabilities of an industrial MEMS SOI process for the fabrication and in developing the read-out electronics. Moreover, the evaluation of the whole set of devices of the design N°1 allows us to collect information and to make recommendations that have been used to design the next generations of MEMS (design N°2). Deep Level Transient Spectroscopy (DLTS) measurements applied on the new devices showed resonance frequencies of about 3 kHz, which makes it possible to have AC voltage references working from about 30 kHz. The stability of the MEMS output voltage at 100 kHz has been found very promising for the best samples where the relative deviation from the mean value over almost 12 hours showed a standard deviation of about 6.3 ppm, which can be considered as a very good result. The assessment of these MEMS devices allowed to understand the larger discrepancies observed when the measurements are carried out over longer times, which have been identified as a result of a mismatch between the vertical motion chosen for the movable electrode and the dimensional characteristics of the SOI wafer imposed by the industrial Tronic's process. Consolidated architectures based on split fingers MEMS showing voltage reference stability as high as 1 ppm at 100 kHz over more than 150 hours.

Acknowledgments

The authors are grateful to Tronic's Microsystems for the fabrication of MEMS devices of high quality, for their constant support, advices and availability.

References

[1]. B. P. van Drieënhuizen, Integrated Electrostatic RMS to Converter , Ph. D. dissertation, *Delft Univ.,* Delft, The Netherlands, 1996.

[2]. B. P. van Drieënhuizen and R. F. Wolffenbuttel, Integrated Micromachined Electrostatic True RMS-to-DC Converter, *IEEE Trans. Instrum. Meas.*, Vol. 44, No. 2, 1995, pp. 370-373.

[3]. M. Suhonen, H. Seppä, A. S. Oja, M. Heinilä, and I. Näkki, AC and DC Voltage Standards Based on Silicon Micromechanics, in Digest, *CPEM'98,* Washington DC, July 1998, pp. 23-24.

[4]. A. Kärkkäinen, N. Pesonen, M. Suhonen, A. Oja, A. Manninen, N. Tisnek, and H. Seppä, MEMS based AC Voltage Reference, *IEEE Trans. Instrum. Meas.,* Vol. 54, Apr. 2005, pp. 595-599.

[5]. A. Kärkkäinen, S. A. Awan, J. Kyynäräinen, P. Pekko, A. Oja, and H. Seppä, Optimized Design and Process for Making a DC Voltage Reference Based on MEMS, *IEEE Trans. Instrum. Meas.,* Vol. 54, Apr. 2005, pp. 563-566.

[6]. Cretu, E., Rocha, L. A. and Wolffenbuttel, R. F. Micromechanical Voltage reference Using the Pull-In of a Beam, *IEEE Trans. Instrum. Meas.*, Vol. 50, Dec. 2001, pp. 1504 -1507.

[7]. J. Kyynäräinen, A. S. Oja, and H. Seppä, A Micromechanical RMS-to-DC Converter, in Digest, *CPEM'2000,* Sydney, May 2000, pp. 699-700.

[8]. G. de Graaf, M. Bartek, Z. Xiao, C. J. van Mullem, and R. F. Wolffenbuttel, Bulk Micromachined Electrostatic True RMS-to-DC Converter, *IEEE Trans. Instrum. Meas.,* Vol. 50, No. 6, Dec. 2001, pp. 1508-1512.

[9]. H. Seppä, J. Kyynäräinen, and A. Oja, Microelectromechanical Systems in Electrical Metrology, *IEEE Trans. Instrum. Meas.,* Vol. 50, No. 2, Apr. 2001, pp. 440-444.

[10].J. Kyynäräinen, A. S. Oja, and H. Seppä, Stability of Microelectromechanical Devices for Electrical Metrology, *IEEE Trans. Instrum. Meas.,* Vol. 50, No. 6, Dec. 2001, pp. 1499-1503.

[11].L. J. Fernandez, E. Visser, J. Sesé, R. J. Wiegerink, H. V. Jansen, J. Flokstra and M. Elwenspoek, Development of a capacitive MEMS RF power sensor without dissipative losses: towards a new philosophy of RF power sensing, *CPEM' 04,* London, UK, June 27 – July 2, 2004.

[12].L. J. Fernandez, E. Visser, J. Sesé, R. J. Wiegerink, H. V. Jansen, J. Flokstra and M. Elwenspoek, Capacitive rf power sensor based on MEMS technology, in *Proc. of the IEEE Sensors Conference,* Toronto, October 22-24, 2003.

[13].A. Alastalo, J. Kyynäräinen, H. Seppä, A. Kärkkäinen, N. Pesonen, M. Lahdes, T. Vähä-Heikkilä, P. Pekko, and J. Dekker, Wideband microwave power sensor Based on MEMS technology, *CPEM'04,* London, UK, June 27 – July 2, 2004.

[14].P. B. Chu, K. S. J. Pister, Analysis of closed-loop control of parallel-plate electrostatic microgrippers, in *Proc. IEEE Int. Conf. Robotics and Automation,* San Diego, CA, May 1994.

[15].J. I. Seeger, S B. Crary, Stabilization of electrostatically actuated mechanical devices, *in Proc. Transducers'97,* Chicago, IL, June 1997.

[16].E. K. Chan and R. W. Dutton, electrostatic micromechanical actuator with extended range of travel, *J. Microelectromechan. Syst.,* Vol. 9, 2000, pp. 321-328.

[17].J. I. Seeger and B. E. Boser, Charge Control of Parallel-Plate, Electrostatic Actuators and the Tip-In Instability, *Journal of Microelectromechanical Systems,* Vol. 12, No. 5, Oct. 2003, pp. 116.

[18].J. I. Seeger and B. E. Boser, Dynamics and control of parallel-plate actuators beyond the electrostatic instability, in *Proc. of the 10th Int. Conf. On Solid-state Sensors and Actuators,* Sendai, Japan, June 7-10, 1999.

[19].R. Nadal-Guardia, A. Dehé, R. Aigner, and L. M. Castañer, Current Drive Methods to Extend the Range of Travel of Electrostatic Microactuators Beyond the Voltage PullIn Point, *Journal of Microelectromechanical Systems,* Vol. 11, No. 3, June 2002, pp. 255-263.

[20].EMMA project report, Information Societies Technology, IST200028261EMMA, 2005.

[21].A. Kärkkäinen, N. Tisnek, A. Manninen, N. Pesonen, A. Oja, and H. Seppä, Electrical stability of a MEMS-based AC voltage reference, *Sensors & Actuators A*, 137, 2007, pp. 169-174.

[22].A. Bounouh, H. Camon, T. Ricart, R. Plana, C. Pisella, F. Ziade, A. Polletaef, D. Allal, D. Leprat, Electrostatic actuated MEMS for precision AC voltage reference, in *Proc. of the Conference on Precision Electromagnetic Measurements (CPEM'2008),* Broomfield-USA, June 2008.

[23].A. Bounouh, H. Camon, D. Bélières, F. Blard, F. Ziade, MEMS AC voltage reference for miniaturized instrumentation and metrology, *Computer Standards & Interfaces,* in Press 2010.

[24].H. Camon, C. Ganibal, Advantages of alternative actuating signal for MEMS actuators, *Sensors & Actuators A*, 136 N°1, 2007, pp. 299-303.

Guide for Contributors

Aims and Scope

Sensors & Transducers Journal (ISSN 1726-5479) provides an advanced forum for the science and technology of physical, chemical sensors and biosensors. It publishes state-of-the-art reviews, regular research and application specific papers, short notes, letters to Editor and sensors related books reviews as well as academic, practical and commercial information of interest to its readership. Because it is an open access, peer review international journal, papers rapidly published in *Sensors & Transducers Journal* will receive a very high publicity. The journal is published monthly as twelve issues per annual by International Frequency Association (IFSA). In additional, some special sponsored and conference issues published annually. *Sensors & Transducers Journal* is indexed and abstracted very quickly by Chemical Abstracts, IndexCopernicus Journals Master List, Open J-Gate, Google Scholar, etc.

Topics Covered

Contributions are invited on all aspects of research, development and application of the science and technology of sensors, transducers and sensor instrumentations. Topics include, but are not restricted to:

- Physical, chemical and biosensors;
- Digital, frequency, period, duty-cycle, time interval, PWM, pulse number output sensors and transducers;
- Theory, principles, effects, design, standardization and modeling;
- Smart sensors and systems;
- Sensor instrumentation;
- Virtual instruments;
- Sensors interfaces, buses and networks;
- Signal processing;
- Frequency (period, duty-cycle)-to-digital converters, ADC;
- Technologies and materials;
- Nanosensors;
- Microsystems;
- Applications.

Submission of papers

Articles should be written in English. Authors are invited to submit by e-mail editor@sensorsportal.com 8-14 pages article (including abstract, illustrations (color or grayscale), photos and references) in both: MS Word (doc) and Acrobat (pdf) formats. Detailed preparation instructions, paper example and template of manuscript are available from the journal's webpage: http://www.sensorsportal.com/HTML/DIGEST/Submition.htm Authors must follow the instructions strictly when submitting their manuscripts.

Advertising Information

Advertising orders and enquires may be sent to sales@sensorsportal.com Please download also our media kit: http://www.sensorsportal.com/DOWNLOADS/Media_Kit_2009.pdf